Low-Power Transimpedance Amplifier for Near Infrared Spectroscopy

Mohamed Atef [1], Ahmed Atef [2], Mohamed Abbas[3]
[1]School of Microelectronics, Shanghai Jiao Tong University, Shanghai, China
[1,3]Electrical Engineering Department, Assiut University, Assiut, Egypt.
[2]Electrical Engineering Department, Sohag University, Sohag, Egypt.
[3] Electronics and Communications Department,Egypt-Japan University of Science and Technology,Alexandria,Egypt
[1]moh_atef@aun.edu.eg, [2] ahmed.atef@eng.sohag.edu.eg, [3]m-abbas@aun.edu.eg

***Abstract*— This paper presents the design and the post layout simulation of a high-sensitivity low-power Transimpedance Amplifier (TIA) for frequency domain functional Near Infrared Spectroscopy (FD-fNIRS). It consumes 194 µW from 1.2 V DC supply. This low power will increase the battery life of the NIRS portable system. The proposed TIA achieves 103.3 dBΩ transimpedance gain, 22 MHz bandwidth and 6.3 nA integrated input noise current using a photodiode with 2 pF capacitance. The demonstrated TIA is simulated using 130 nm CMOS technology occupying an area of 0.0012 mm^2. Post amplifier stages are presented to increase the total gain and to interface the ADC in the next stage. The complete receiver achieves 120.6 dBΩ gain, 19.9 MHz bandwidth, 6.6 nA total input noise and consumes 2.4 mW from 1.2 V DC supply.**

***Keywords- Near Infrared spectroscopy (NIRS) ,Optical Receiver, Transimpedance Amplifier (TIA)*.**

I. INTRODUCTION

Near Infrared Spectroscopy (NIRS) is used in biomedical applications as an oxygen concentration based imaging technique. NIRS monitors the Oxygen, Hemoglobin (He) and Deoxy Hemoglobin (DeHe) in human organs like brain, bladder, and muscles [1]. Light wavelengths in the NIR range can penetrate tissues to few centimeters [2]. In this regard optical transceivers that operate from 600 nm to 950 nm receive great research interest. The optical transmitter sends NIR light signal through the skull and optical receiver detects and amplifies the reflected weak light signal, then the blood features like O_2, He, and DeHe can be extracted. Using NIRS to measure the hemoglobin concentration and oxygen saturation enables cancer detection [3]. NIRS is used to identify vulnerable periods for the development of neurological injury after paediatric cardiac surgery [4].

There are three major types of NIRS devices, continuous wave (CW), time domain (TD) and frequency domain (FD) [5]. CW type is the most simple and the least complex technique. It monitors the decay of the reflected signal when it reflects back from the tissues and hence determines oxygen saturation. On the other hand, The FD type provides more accurate results and extracts more features. In the FD type the frequency content, phase change, and amplitude attenuation of the reflected signal are monitored to extract blood features. However, its sensitivity is affected by the uncertainty in phase calculations. TD monitors the returned pulse broadening and measures the time of the flight of the returned pulse [5] making it the most expensive and complex technique.

One of the advantages of NIRS is its ability to provide a portable system. As a result, the system requires small chip area, low power consumption and limited emitted optical power for safety. Exposure to laser is limited to a 329 mJ/cm^2 according to American National Standards Institute (ANSI) [6]. Accordingly, reflected optical power from tissues is limited to less than one microwatt [3]. This demonstrates the need of high sensitivity and high gain NIRS optical receivers. Choosing the suitable design parameter for NIRS optical receiver front end TIA is very critical and affects the overall system performance. NIRS system uses an array of optical receiver (photodiode and TIA) and transmitter (laser diode and its driver) pair called an optode.

A block diagram of the FD-NIRS transceiver is shown in Figure 1. A sinusoidal source generates a signal fed to the laser driver. The transmitted optical signal follows a banana shape when propagating through the skull and brain tissues. An optical receiver senses the reflected optical signal, amplifies and filters it. Then the amplified signal is fed to the next phase resolving stage and Analog to Digital Converter (ADC). For FD-NIRS, the optical receivers' bandwidth and power consumption implies a compromise. The average time taken from the source to the detector for human skull is around 1 ns for 720 nm NIR light [7]. This experienced 1 ns signal delay requires that the next phase resolving circuit must be able to extract that small delay.

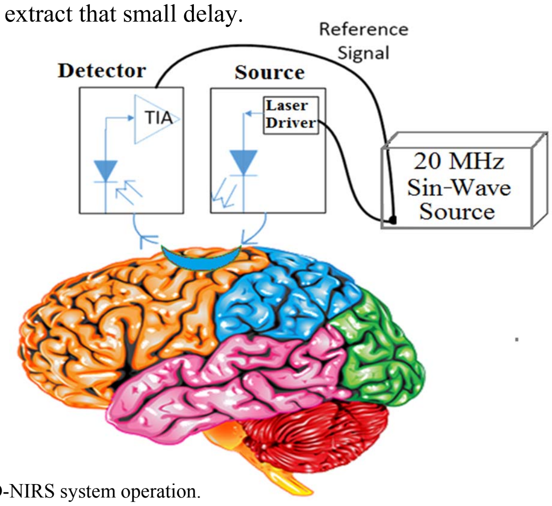

Fig.1 FD-NIRS system operation.

978-1-4799-5341-7/16/$31.00 ©2016 IEEE

On one hand, enhancing the resolution of the phase resolving stage can be done by increasing the signal operating frequency. But this on the other hand requires higher receiver bandwidth which result in higher total input referred noise, higher power consumption, lower gain and a reduced sensitivity. TIAs with higher input noise needs extra laser emitted optical power which is limited due to the safety regulations specified by ANSI [6].

This paper will be organized as follows. The first section describes the proposed high sensitive, low power TIA architecture and mathematical analysis. The second section introduces a post layout simulation results and discussion. Finally a comparison with state of the art NIRS TIAs is presented.

II. CIRCUIT ANALYSIS

The circuit diagram of the proposed TIA is shown in Figure 2. It is consisting of two stages, regulated cascode (RGC) input stage [8] and an inverter cascode based output stage [9]. The RGC low input impedance serves to increase bandwidth. The high open loop gain and the high output impedance of the inverter cascode stage (M_{n1}, M_{n2}, M_{p1}, M_{p2}) serves to increase the transimpedance gain. The cascode transistor M_{n2} is biased by the output of the regulating inverter amplifier of RGC which eleminate the need of extra biasing source and PAD. The input photocurrent coming from the photodiode is fed to the RGC input stage,which acts as a current buffer having input impedance of $((1/SC_{PD})//(1/G_{mcasc}))$ where $1/G_{mcasc}$ is the RGC input resistance.

This small input resistance increases the bandwidth by isolating the high input photodiode capacitance [8]. The current I_x coming from RGC stage is then fed to the input of the output stage which amplifies and converts I_x to an output voltage V_{out}.

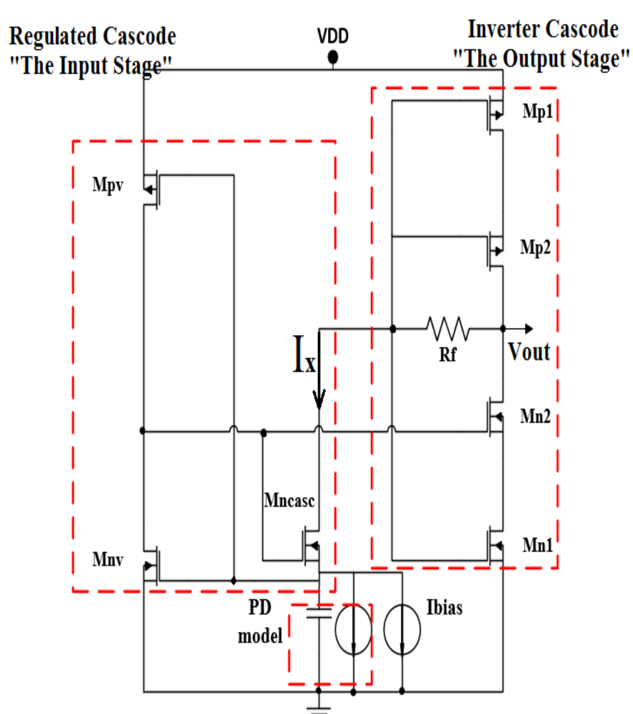

Fig.2 The proposed high sensitivity TIA

Transistors M_{n1}, M_{n2}, M_{p1}, M_{p2} are biased in the weak inversion region. This ensures low power consumption and high drain-source resistance and hence higher open loop gain.

A. The TIA Input Stage

An inverter based amplifier acts as a regulating amplifier to further increase the effective transconductance of the input NMOS [10]. The effective transconductance G_{mcasc} for the RGC input stage can be described by:

$$G_{mcasc} = g_{mcasc}[(g_{mnv} + g_{mpv}).r_{onv}//r_{opv}] \quad (1)$$

where G_{mcasc} is the effective transconductance of the RGC , g_{mcasc} is the transconductance of "M_{ncasc}" transistor. The transfer function of RGC is given by :

$$\frac{I_X}{I_{PD}} = \frac{G_{mcasc}}{(SC_{PD} + G_{mcasc})(SC_i R_{Casc} + 1)} \quad (2)$$

where C_i, R_{Casc} are respectively the capacitance and the resistance seen by the RGC at the inverter cascode input which is described by:

$$R_{Casc} = \frac{R_F + R_{out}}{A_{invc} + 1} \quad (3)$$

Also I_x is denoted on Figure 2, I_{PD} , C_{PD} are the photodiode input current and junction capacitance respectively .
$R_{out} = (g_{mn1}.r_{op1}.r_{on1}//g_{mn2}.r_{op2}.r_{on2})$ and $A_{invc} = (g_{mn1} + g_{mp1}).R_{out}$. are respectively the output resistance and the open loop gain of the inverter cascode output stage.

B. TIA Output Stage

The output stage is an inverter cascode based TIA that amplifies the current coming from the RGC and convert it to a voltage according to:

$$Z_{invc}(S) = \frac{V_{out}}{I_X} = \frac{R_F A_{invc}}{S^2(C_i C_{out} R_F R_{out}) + S([R_F + R_{out}]C_i + R_{out}C_{out}) + A_{invc}} \quad (4)$$

Where C_{out} is the capacitance at the TIA output node. By realizing that the total transimpedance transfer function is the multiplication of equation 2 and 4 which yields:

$$Z_{TIA}(S) = \frac{V_{out}}{I_{PD}} = \frac{R_F}{\left(\frac{S\,C_{PD}}{G_{mcasc}} + 1\right)\left(SC_i \frac{R_{out} + R_F}{A_{invc} + 1} + 1\right)\left(\frac{S\,R_{out} C_{out}}{A_{invc}} + 1\right)} \quad (5)$$

Equation 5 reveals that the pole presented due to inverter cascode input impedance can be controlled by increasing A_{invc} and realizing that $C_i << C_{PD}$ so that:

$$\frac{G_{mcasc}}{C_{PD}} \ll \frac{A_{invc}}{C_i\,(R_F + R_{out})} \quad (6)$$

Inequality 6 reveals that the total bandwidth is almost determined by the dominant pole due to the RGC stage and the isolation of high photodiode input capacitance is accomplished.

$$BW = \frac{G_{mcasc}}{2\,\pi\,C_{PD}} \quad (7)$$

C. Post amplifier

The output of the TIA is fed to a single ended to differential stage [8] to suppress supply noise and enhance the common mode rejection. A two stage differential amplifier as shown in Fig. 3 is used to enhance the gain. Input from the TIA is fed directly to transistor “M_{n3}” and fed via a low pass filter to transistor “M_{n4}” to achieve the single to differential conversion.

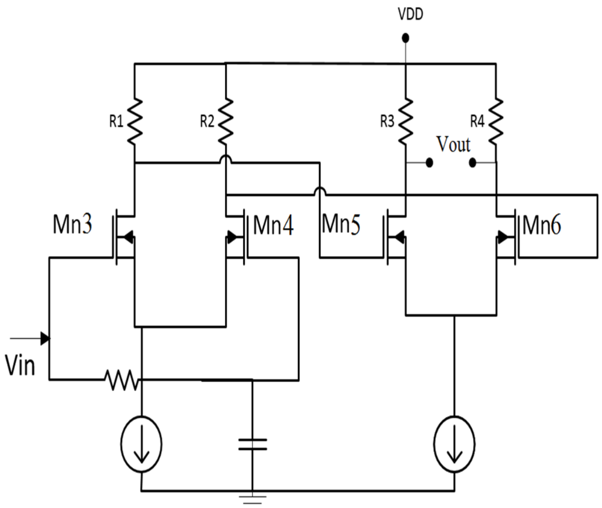

Fig.3 Single ended to differential conversion and post amplifier

III. POST LAYOUT SIMULATION RESULTS AND DISCUSSION

The post layout simulation is performed using Spectre under Cadence. The complete optical receiver is simulated using 130 nm CMOS technology. The complete chip with PADs and ESD is shown in Fig.4. The following post layout simulation results include PADs and ESD protection circuitry. Bonding wires are accounted for and are modeled by 0.5 nH inductor.TIA is optimized for 2 pF off-chip PIN photodiode.

The frequency response of the proposed TIA together with the complete receiver frequency response is shown in Figure 5. The TIA has 22 MHz bandwidth. The complete receiver has a low cutoff frequency at 35 KHz due to single to differential

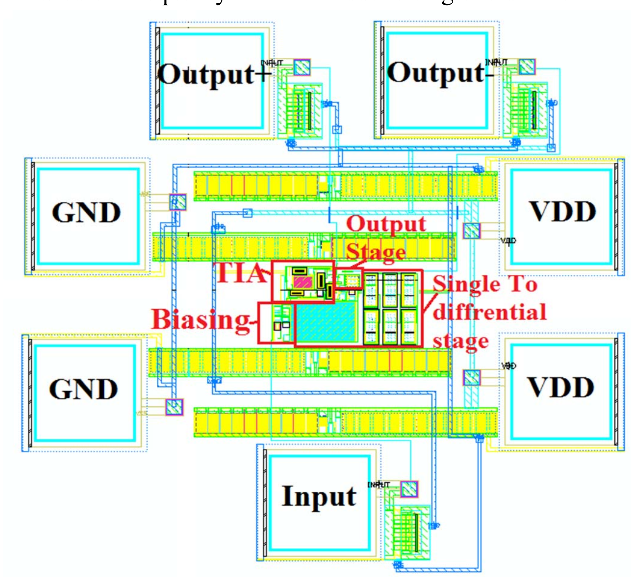

Fig.4 The complete optical receiver with biasing and PADs.

conversion and a bandwidth of 19.9 MHz. For the TIA a 103.3 dBΩ gain and 6.4 nA_{rms} are achieved to ensure high sensitivity. The simulation results show that the RGC input stage consumes 74 µW while the inverter cascode TIA output stage consumes 120 µW. The inverter cascode core amplifier achieves 200 MHz bandwidth which is much larger than the closed loop bandwidth to ensure stability [11]. The complete receiver has an extra 17.3 dBΩ provided by the post amplifier stages. Input referred noise current spectral density of the complete receiver is shown in Figure 6. The average input noise current spectral density is 1.8 pA/sqrt(Hz) in the bandwidth of interest.

The 1 dB compression point and Total Harmonic Distortion (THD) provide an insight of the maximum overloading peak-peak input current. THD of the complete receiver and the TIA is shown in Figure 7. A THD of 5% occurs at 2.8 $\mu A_{p\text{-}p}$ input photocurrent for the TIA and at 1.3 $\mu A_{p\text{-}p}$ for the complete receiver. The proposed TIA exhibits a 1 dB compression point at 3.5 $\mu A_{p\text{-}p}$ input current. Post layout simulation shows a maximum overloading input current of 1.6 $\mu A_{p\text{-}p}$. The small total input referred noise, THD and 1 dB compression point shows the wide input dynamic range of the TIA which is necessary for NIRS application. The post amplifier consumes 1.85 mW from a 1.2 V DC supply and increases the gain of the complete receiver to 120.6 dBΩ. Output driver has a 500 Ω output resistance to interface the next ADC stage. The output driver consumes 1.56 mW from 1.2V DC voltage source which is around 84.3% of the total power consumption.

Monte-Carlo simulation is done using 1000 runs for the proposed TIA to estimate the effect of process variation. Standard deviation and average values of the DC current consumption, bandwidth and gain are shown in Fig.8.

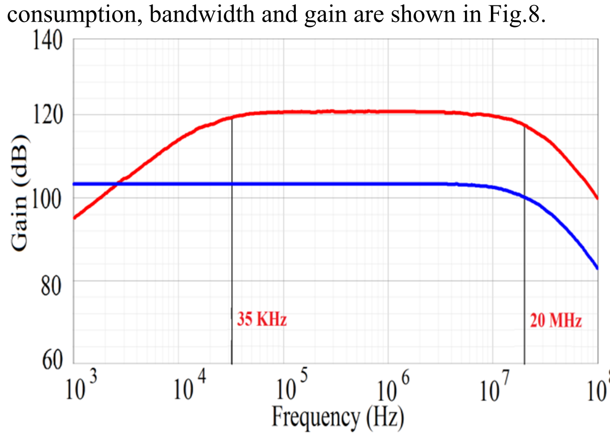

Fig.5 Frequency response of the TIA and the complete receiver

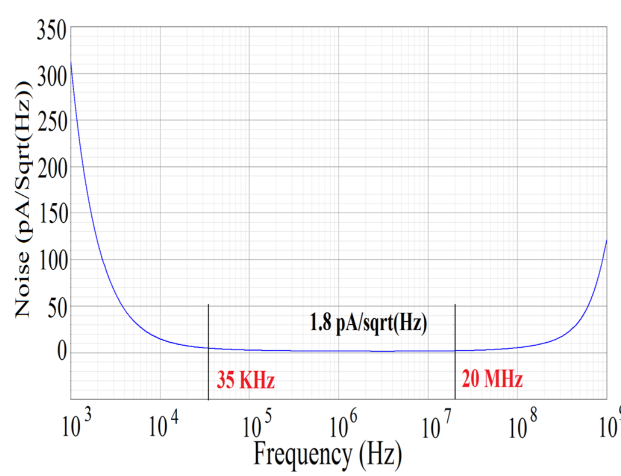

Fig.6 Input current noise density of the complete receiver

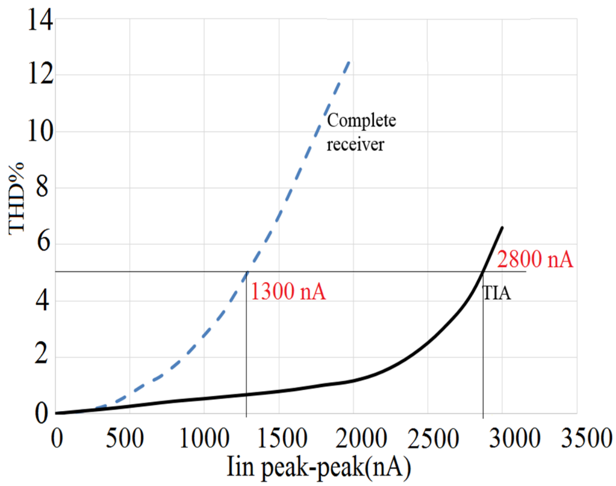

Fig.7 THD of the TIA and the complete receiver

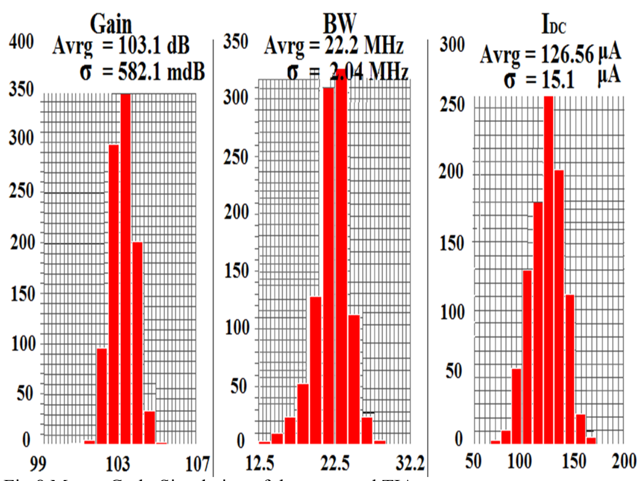

Fig.8 Monte-Carlo Simulation of the proposed TIA

The simulation results show an average gain of 103.15 dBΩ and 0.582 dBΩ standard deviation. For the bandwidth an average value of 22.2 MHz with 2.04 MHz standard deviation. An average 126.56 µA biasing current is recorded with15.1 µA standard deviation.

The Figure of Merit introduced in [8] offers a good and widely used way to compare different TIA topology which is described by:

$$\mathrm{FoM} = \frac{\mathrm{Gain\ (K\Omega).\ BW\ (MHz)\ .\ C\ (pF)}}{\mathrm{Power\ \ Dissipation\ (mW)\ .\ Input\ noise\ (nA)}} \quad (8)$$

Table.I compares this work along with previously published NIRS TIAs used for biomedical applications. References which introduce simulation results are selected for fair comparison [10-13]. It's clear that the proposed TIA achieves the highest FoM and the lowest power consumption. The design proposed in [10] achieves the highest bandwidth at the cost of higher input referred noise and the highest power consumption. The TIA introduced in [11] offers high GBW at the expense of higher input referred noise. The design introduced in [12] operates at large input capacitance with a better sensitivity but the bandwidth is limited to 40kHz.The TIA introduced in [13] achieves a better gain and lower noise, however, its power consumption is much higher than our proposed design.

TABLE I COMPARISON WITH NIRS TIAS

Design	This Work	[10]	[11]*	[12]	[13]
Technology(nm)	130	180	180	180	180
Capacitance(pF)	2	1.5	4	12	2(Assumed)
TIA gain(dBΩ)	103.3	100	107	95	104.1
TIA BW(MHz)	22	280	200	0.04	19
TIA input noise current	6.4nA, 1.8pA/√Hz	85nA -------	158nA -------	1.4nA, 3pA/√Hz	2.1nA , 500fA/√Hz
TIA power (mW)	0.194	22.5	12.3	0.3	0.71
FoM	4828	21.96	92	65.2	4128

*Measured.

IV. CONCLUSION

A novel TIA design along with analysis and post layout simulation results is presented. The proposed TIA achieves the essential low power consumption required for portable fNIRS. The low THD together with the high sensitivity reveals the wide input dynamic range of the TIA. The complete optical receiver is suitable for high resolution phase-resolving FD-NIRS.

ACKNOWLEDGEMENT

This research is sponsored in part by Chinese National 973 Program under Grant 2013CB329401 and in part by the Science and Technology Commission of Shanghai Municipality under Grant 14511100300.

REFRENCES

[1] A. Gersten, J. Perle, A. Raz, R. Fried, "Probing Brain Oxygenation with Near Infrared Spectroscopy" Neuro Quantology, vol 7, no. 2, PP.258-266, 2009.

[2] FF. Jobsis , "Noninvasive Infrared Monitoring of Cerebral Andmyocardial Oxygen Sufficiency and Circulatory Parameters". Science, vol. 198, no. 4323, pp.1264-1267, 1977.

[3] S. Srinivasan, C. Carpenter, and B.W. Pogue, "Sensitivity of Hemoglobin Concentration on Optical Probe Positioning in Image-guided Near Infrared Spectroscopy" International Conference of the IEEE Engineering in Medicine and Biology Society, pp.1994–1996, 2009.

[4] P.E.F. Daubeney, D.C. Smith, S.N. Pilkington, R.K. Lamb, J.L. Monro, V.T. Tsang, S.A. Livesey, and S.A. Webber, "Cerebral oxygenation during paediatric cardiac surgery: identification of vulnerable periods using near infrared spectroscopy." European Journal of Cardio-Thoracic Surgery , vol. 13 , no. 4 , pp. 370-377, 1998.

[5] A. Bakker, B. Smith, P. Ainslie, and K. Smith,"Near Infrared Spectroscopy, Applied Aspects of Ultrasonography in Humans, Prof. Philip Ainslie (Ed.)" , ISBN 978-953-51-0522-0, InTech, 2012.

[6] American National Standards for The Safe Use of Laser, American National Standards Institute, New York, Z136.1 , 2007.

[7] D. T. Delpy, M. Cope, P. van der Zee, S. Arridge, S. Wray, and J. Wyatt, "Estimation of Optical Pathlength through Tissue from Direct Time of Flight Measurement" Physics in Medicine and Biology, vol. 33 , no. 12, pp.1433-144 , 1988.

[8] M.Atef, H.Zimmermann, " Low-Power 10 Gb/s Inductorless Inverter Based Common-Drain Active Feedback Transimpedance Amplifier in 40 nm CMOS" Springer Analog Integr. Circ. Sig. Processing, vol.76, no.3, pp. 367-376, 2013.

[9] M. Atef, H. Zimmermann, "10Gb/s Inverter Based Cascode Transimpedance Amplifier in 40nm CMOS Technology" , IEEE DDECS Int. Conf., pp.72 – 75, Karlovy Vary, 2013.

[10] Ruida Yun and Valencia M. Joyner, "A Monolithically Integrated Phase-Sensitive Optical Sensor for Frequency-Domain NIR Spectroscopy", IEEE Sensor Journal, vol. 10, no. 7, pp.1234-1242 ,2010.

[11] R. Yun, V. Koomson "A Novel CMOS Frequency-Mixing Transimpedance Amplifier for Frequency Domain Near Infrared Spectroscopy " , TCAS–I ,vol. 60, no. 1, pp. 84-94, 2013.

[12] F. Normandin, M. Sawan, and J. Faubert, "A New Integrated Front-End for a Noninvasive Brain Imaging System Based on Near-Infrared Spectroreflectometry", TCAS-I, vol. 52, no. 12, pp.2663-2671, 2005.

[13] A. Chaddad, "Low-Noise Front-End Receiver Dedicated to Biomedical Devices: NIRS Acquisition System" Circuits and Systems, vol.5, pp.191-200, 2014.